How to compute the land cover evapotranspiration at regional scale? A spatial approach of Emilia-Romagna region

Mircea-Mărgărit NISTOR[1]* and Ghiurco Cosmin Gabriel PORUMB[2]

[1] Department of Chemical and Geological Sciences, University of Modena and Reggio Emilia, Via Campi No. 103, 41125, Modena, Italy

[2] Human Geography and Tourism Department, Faculty of Geography, Babeș-Bolyai University, Cluj-Napoca, Romania

* Correspondence to: Mircea-Mărgărit NISTOR, University of University of Modena and Reggio Emilia, Modena, Italy. E-mail: renddel@yahoo.com.

doi: 10.4316/GEOREVIEW.2015.25.1.268

GEOREVIEW

Article history
Received: April 2015
Received in revised form: July 2015
Accepted: August 2015
Available online: September 2015

ABSTRACT: The Earth is rapidly changing in both its climate and its land distribution. The numerous methods from the literature show various possibilities to assess the crop evapotranspiration and evaporation rate, both with direct measurements and empirical formulas. The present paper brings forward a methodology that demonstrates how to compute the potential land cover evapotranspiration (ET_c) at regional scale using climate data from 13 meteorological stations, empirical equations, Corine Land Cover data, and the Geographical Information System (GIS). Based on Thornthwaite method and evapotranspiration coefficients, the study assesses the ET_c of Emilia-Romagna region in four stages. Moreover, the Budyko approach was applied to calculate the actual evapotraspiration (AET_0) and actual land cover evapotranspiration (AET_c) to identify the critical areas of water deficit. Po Plain represents an area with high evapotranspiration rate, due to temperatures and cultivation patterns. A value of 778.87 mm/year at Ferrara station was calculated for the potential evapotranspiration (ET_0), while the ET_c ranging to 800-1000 mm/year in the central and northeastern part of the region. The AET_c reached the maximum values of 724 mm in the southcentral part of the Emilia-Romagna.

KEY WORDS: land cover evapotranspiration, climate change, spatial distribution, water balance, Emilia-Romagna

1. Introduction

Water has become a precious resource in the 21st century due to global climate changes. The observed changes in freshwater resources occur due to runoff reductions in rivers, earlier annual peak discharges, melting glaciers, decreased recharge of karst aquifers, and decreased groundwater recharge (Collins, 2008; Aguilera and Murillo, 2009; Hidalgo et al., 2009; Piao et al., 2010; Jiménez Cisneros et al., 2014). Climate change influence can be seen on surface waters and groundwaters (Loàiciga et al., 2000; Bachu and Adams, 2003; Brouyère et al., 2004).

In the last century registered essentials data was recorded showing a rising in temperature (IPCC, 2001) and a decrease in precipitation. The climate is warming (Shaver et al., 2000; Oerlemans, 2005; Dong et al., 2013; Xie et al., 2013) and, due to this, regional climate conditions are changing from place to place, precipitation quantity is decreasing and the future projections show a downtrend for precipitation and an increase in mean temperature up to 3°C (Stocks et al., 1998; Stavig et al., 2005; The Canadian Centre for Climate Modelling, 2014). The report IPCC (2007) also shows that melting of permafrost may contribute to climate warming. Furthermore, global population growth has led to a need for higher quantity of food products, which require a greater amount of water resources. Evapotranspiration plays an important role in the water balance of a region. Due its importance, evapotranspiration has become a useful parameter for a wide area of interest: hydrology, agriculture, climate change, and botany.

Until now, studies on ET_0 variation and AET_0 and its impact on agriculture and water balance have been conducted by Allen (2000), Gowda et al. (2008), Geritts et al. (2009). Prăvălie et al. (2014) assessed the evapotranspiration based on satellite data in aim to detect the aridization in Oltenia region. The water balance for China over 1960-2002 through calculation of actual evapotranspiration was made by Gao et al. (2007), Gao et al. (2012). They argued in their studies about Haihe River basin from China that actual evapotranspiration is a useful indicator for changes of water cycle and climate. In the speciality literature there are a number of papers that claim that the negative impact of climate change can be seen on ecosystems and on groundwater recharge (Parmesan and Yohe, 2003; Campos et al., 2013; Prăvălie et al., 2014).

Recently, Mojid et al. (2015) argued that climate change impacts contribute to crop-water demand. Prăvălie (2014), IPPC (2007) recall that evapotranspiration at global scale is related to the trend in temperature and anthropogenic complex factors. As mentioned by Chen et al. (2006), Kousari et al. (2013) reported that the evapotranspiration is the third important climatic factor that controls the terrestrial ecosystems and the atmosphere mass exchange. Thus, the assessment of ET_c becomes a significant indicator that is used commonly in regional water balace and irrigation surveys. Kurnik et al. (2014), in their study about water deficit in agricultural regions of Europe, created a soil water balance model that included simulations of soil water deficit and actual evapotranspiration.

The Emilia-Romagna constitutes the most important agricultural and industrial region in Italy and the land cover of this region has experienced a major change in the last decade. Water demand is vital not only for the region's progress, but also for the entire country. For this reason, our study proposes an integrated methodology which predicts the spatial ET_c of Emilia-Romagna region based on average climate data over the fifteen years and Corine Land Cover 2006 (CLC2006). The spatial distribution of temperature, precipitation, ET_0, land cover coefficient (K_{clc}), AET_0, and the AET_c on Emilia-Romagna regional map were performed using the ArcGIS 10.2.2 software from ESRI.

2. Study area

Emilia-Romagna region is located in the northern part of Italy (Figure 1) and extends on the Po Plain and Northern Apennines. Confirmed by ISTAT (2014), in 2012 Emilia-Romagna was the first region in Italy with food products of PDO (Protected Designation of Origin), PGI (Protected

Geographical Indication), and plant protection products used for the protection of agricultural crops.

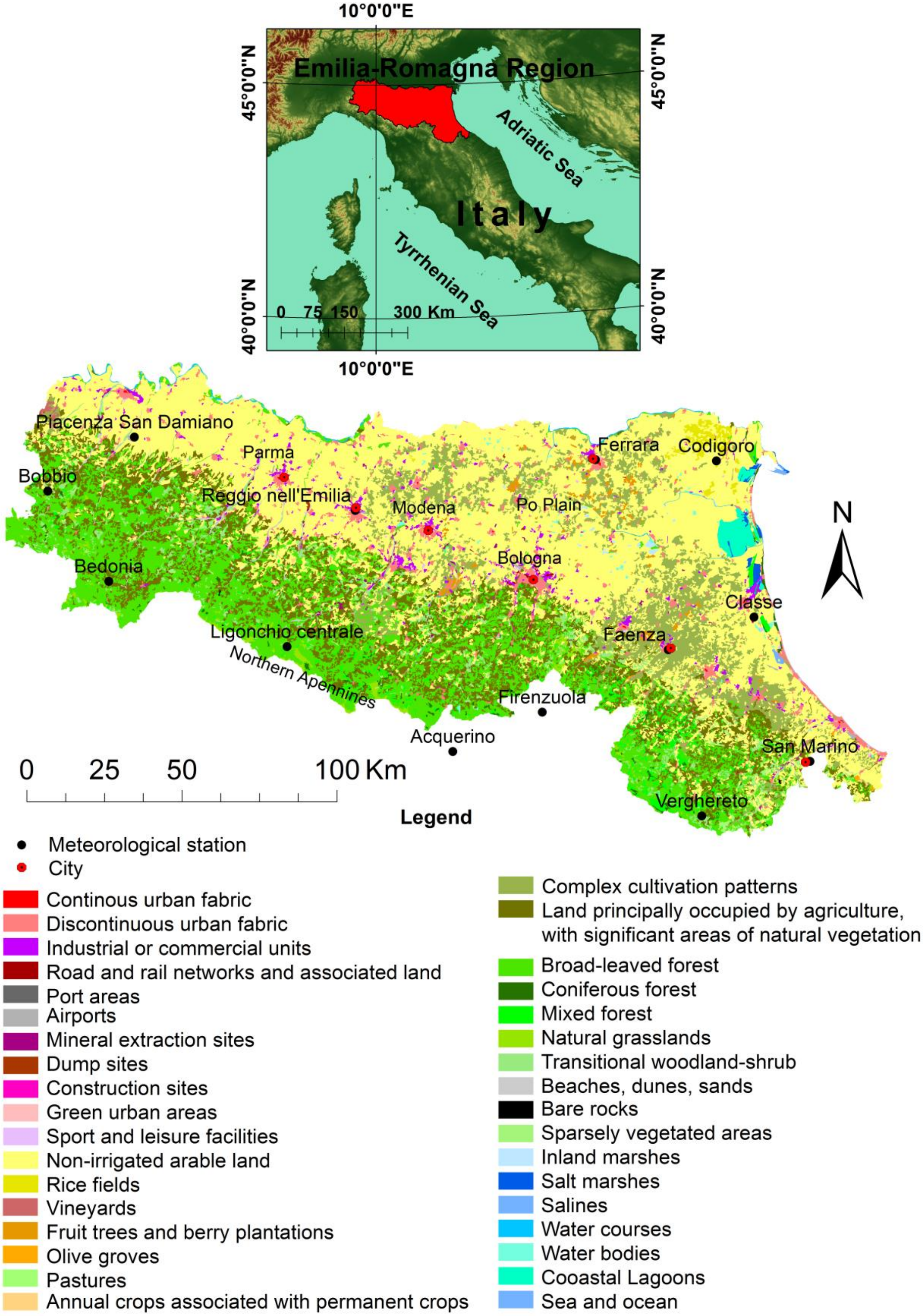

Figure 1 Land cover of Emilia-Romagna region and location of study area on Italy map.

The geomorphology of the Emilia-Romagna region, divided in three relief units and disposed in parallel lines to northwest to southeast, is highly reflected in the climate of the region. The high altitudes of Northern Apennines (2165 m Cimone Mount) have an important role in spatial variation of the precipitation of Emilia-Romagna region, precipitation which exceeds 1600 mm in mountain chain, while in the Po Plain the values of precipitation fall below 800 mm. The Köppen-Geiger climate classification indicates a temperate fully humid climate with hot summers (Cfa) in the northeast part of the region and fully humid climate with warm summers (Cfb) in the southwest part of the region (Kottek et al., 2006).

The land cover of Emilia-Romagna is largery composed of artificial, agricultural and grassland areas in Po Plain, while the coniferous and broad-leaved forests are predominantly in the mountains and hilly area. In the eastern part of the region, on the coastal zone of Adriatic Sea, there are a consistent number of lagoons, inlands, and marshland. The physical aspects of the orography and the actual climate distribution together with arrangement of land cover contribute in different ways to spatial variation of ET_c at regional scale of Emilia-Romagna.

3. Materials and methods

3.1. Climate data

From 1991 to 2005 monthly mean air temperature and precipitation (Arpa Emilia-Romagna, 2015) levels from thirteen meteorological stations (Table 1), situated in Emilia-Romagna and its surroundings, were used to compute the spatial distribution of ET_0 and AET_0 and further ET_c and AET_c in the study area. The seasonal raster map of monthly and annual ET_0 were derived from the monthly mean temperatures and the seasonal maps of ET_c were derived from the land cover data. Integrating the ET_c parameter in the ratio of the aridity index, the Budyko approach was used in the calculation of the AET_c of Emilia-Romagna region.

Table 1 The meteorological stations and their corresponding geographical coordinates (latitude and longitude) and elevations

Station	Longitude (decimal degrees)	Latitude (decimal degrees)	Elevation above mean sea level (m)
Codigoro	12.1	44.83	2
Classe	12.23	44.37	2
San Marino	12.44	43.94	652
Verghereto	12	43.79	812
Firenzuola	11.37	44.11	422
Faenza	11.88	44.28	35
Acquerino	11.01	44	890
Ferrara	11.61	44.84	15
Reggio nell'Emilia	10.63	44.7	51
Bedonia	9.63	44.5	544
Bobbio	9.38	44.76	270
Piacenza San Damiano	9.73	44.92	134
Ligonchio centrale	10.35	44.31	928

3.2. Corine Land Cover 2006 (CLC2006)

CLC2006 is a spatial database that includes the land cover characteristics of the Globe. These characeristics are divided in five main classes: artificial areas, agricultural areas, forests, wet lands, and water bodies. Vector data of CLC2006 for Europe at 4th level dating from 2006 was used to represent the cover layer for entire Emilia-Romagna region. In present study, the elements of CLC2006 are the ratio of ET_c that contains spatial extension of the land cover and crops, but also the land use, water bodies and bare soils of the Emilia-Romagna region. The vector data of CLC2006 was analysed and a K_{clc} coefficient related to FAO Drainage Paper56 (Allen et al., 1998) for the each class of CLC2006 founded in Emilia-Romagna was assigned. Furthermore, the conversion from vector to raster data was done.

3.3. Methods

3.3.1. Thornthwaite method for ET_0 calculation

The method proposed by Thornthwaite (1948) is simple and efficient to use at regional scale due to climatic long period data sets. Thonthwaite equation (Eq. 1) requires average monthly temperatures (T_i) and it provides the monthly ET_0. Input data are based on annual heat index (I) (Eq. (2)) and alfa parameter (α) (Eq. (3)). The method was used in many hydrological studies by McCabe and Wolock (1991), Rosenberry et al. (2007), Rahardjo et al. (2012).

$$ET_0 = 1.6\left(\frac{10\ T_i}{I}\right)^{\alpha}\ [cm/month] \qquad (Eq.1)$$

where:
ET_0 = potential evapotranspiration
T_i = monthly air temperature
α = complex function of heat index
I = annual heat index

$$I = \sum_{i=1}^{12}\left(\frac{T_i}{5}\right)^{1,514} \qquad (Eq.2)$$

where:
Ti = monthly air temperature

$$\propto = 6.75\ \times 10^{-7}I^3 -\ 7.71 \times 10^{-5}I^2 + 1.7912\ \times\ 10^{-2}I + 0.49239 \qquad (Eq.3)$$

where:
I = annual heat index

3.3.2. Land cover evapotranspiration (ET_c)

The evapotranspiration rate due by the plants is called crop evapotranspiration (ET_c) (Allen et al., 1998). The most used methodology for ET_c is depicted in FAO Drainage Paper56 and contains the methods to compute the daily ET_0 based on Penman-Montheith equation. The crop coefficient (K_c) for different category of plants are detailed in the same source. The apropriate K_{clc} was assigned for land cover classes using standards values presented by FAO and in specific literature. Land cover of Emilia-Romagna region is composed by a variety of land use and non-cultivated patterns that don't have a standard K_c. The annual variation of the ET_c was analysed, using the K_{clc} for four stages of functionality of crops: initial (from March to May), mid-season (from June to August), end-season or late season (September and October), and cold season (January, February, November, and December).

Table 2 Corine Land Cover coefficients used for ET_c in Emilia-Romagna region

Corine Land Cover		K_{ini} season					K_{mid} season					K_{end} season					K_{cold} season				
CLC2006 code	CLC Description	K_c	K_s	K_u	K_w	K_{clc}	K_c	K_s	K_u	K_w	K_{clc}	K_c	K_s	K_u	K_w	K_{clc}	K_c	K_s	K_u	K_w	K_{clc}
111	Continous urban fabric	-	-	0.2	-	0.2	-	-	0.4	-	0.4	-	-	0.25	-	0.25	-	-	-	-	-
112	Discontinuous urban fabric	-	-	0.1	-	0.1	-	-	0.3	-	0.3	-	-	0.2	-	0.2	-	-	-	-	-
121	Industrial or commercial units	-	-	0.2	-	0.2	-	-	0.4	-	0.4	-	-	0.3	-	0.3	-	-	-	-	-
122	Road and rail networks and associated land	-	-	0.15	-	0.15	-	-	0.35	-	0.35	-	-	0.25	-	0.25	-	-	-	-	-
123	Port areas	-	-	0.3	-	0.3	-	-	0.5	-	0.5	-	-	0.4	-	0.4	-	-	-	-	-
124	Airports	-	-	0.2	-	0.2	-	-	0.4	-	0.4	-	-	0.3	-	0.3	-	-	-	-	-
131	Mineral extraction sites	-	-	0.16	-	0.16	-	-	0.36	-	0.36	-	-	0.26	-	0.26	-	-	-	-	-
132	Dump sites	-	-	0.16	-	0.16	-	-	0.36	-	0.36	-	-	0.26	-	0.26	-	-	-	-	-
133	Construction sites	-	-	0.16	-	0.16	-	-	0.36	-	0.36	-	-	0.26	-	0.26	-	-	-	-	-
141	Green urban areas	-	-	0.12	-	0.12	-	-	0.32	-	0.32	-	-	0.22	-	0.22	-	-	-	-	-
142	Sport and leisure facilities	-	-	0.1	-	0.1	-	-	0.3	-	0.3	-	-	0.2	-	0.2	-	-	-	-	-
211	Non-irrigated arable land	1.1	-	-	-	1.1	1.35	-	-	-	1.35	1.25	-	-	-	1.25	-	-	-	-	-
213	Rice fields	1.05	-	-	-	1.05	1.2	-	-	-	1.2	0.6	-	-	-	0.6	-	-	-	-	-
221	Vineyards	0.3	-	-	-	0.3	0.7	-	-	-	0.7	0.45	-	-	-	0.45	-	-	-	-	-
222	Fruit trees and berry plantations	0.3	-	-	-	0.3	1.05	-	-	-	1.05	0.5	-	-	-	0.5	-	-	-	-	-
223	Olive groves	0.65	-	-	-	0.65	0.7	-	-	-	0.7	0.7	-	-	-	0.7	-	-	-	-	-
231	Pastures	0.4	-	-	-	0.4	0.9	-	-	-	0.9	0.8	-	-	-	0.8	-	-	-	-	-
241	Annual crops associated with permanent crops	0.5	-	-	-	0.5	0.8	-	-	-	0.8	0.7	-	-	-	0.7	-	-	-	-	-
242	Complex cultivation patterns	1.1	-	-	-	1.1	1.35	-	-	-	1.35	1.25	-	-	-	1.25	-	-	-	-	-
243	Land principally occupied by agriculture. with significant areas of natural vegetation	0.7	-	-	-	0.7	1.15	-	-	-	1.15	1	-	-	-	1	-	-	-	-	-
311	Broad-leaved forest	1.3	-	-	-	1.3	1.6	-	-	-	1.6	1.5	-	-	-	1.5	0.6	-	-	-	0.6
312	Coniferous forest	1	-	-	-	1	1	-	-	-	1	1	-	-	-	1	1	-	-	-	1
313	Mixed forest	1.2	-	-	-	1.2	1.5	-	-	-	1.5	1.3	-	-	-	1.3	0.8	-	-	-	0.8
321	Natural grasslands	0.3	-	-	-	0.3	1.15	-	-	-	1.15	1.1	-	-	-	1.1	-	-	-	-	-
324	Transitional woodland-shrub	0.8	-	-	-	0.8	1	-	-	-	1	0.95	-	-	-	0.95	-	-	-	-	-
331	Beaches. dunes. sands	-	0.2	-	-	0.2	-	0.3	-	-	0.3	-	0.25	-	-	0.25	-	-	-	-	-
332	Bare rocks	-	0.15	-	-	0.15	-	0.2	-	-	0.2	-	0.05	-	-	0.05	-	-	-	-	-
333	Sparsely vegetated areas	0.4	-	-	-	0.4	0.6	-	-	-	0.6	0.5	-	-	-	0.5	-	-	-	-	-
411	Inland marshes	-	-	-	0.15	0.15	-	-	-	0.5	0.45	-	-	-	0.8	0.8	-	-	-	-	-
421	Salt marshes	-	-	-	0.1	0.1	-	-	-	0.5	0.45	-	-	-	0.8	0.8	-	-	-	-	-
422	Salines	-	-	-	0.05	0.05	-	-	-	0.3	0.3	-	-	-	0.5	0.5	-	-	-	-	-
511	Water courses	-	-	-	0.25	0.25	-	-	-	0.7	0.65	-	-	-	1.25	1.25	-	-	-	-	-
512	Water bodies	-	-	-	0.25	0.25	-	-	-	0.7	0.65	-	-	-	1.25	1.25	-	-	-	-	-
521	Cooastal Lagoons	-	-	-	0.3	0.3	-	-	-	0.7	0.7	-	-	-	1.3	1.3	-	-	-	-	-
523	Sea and ocean	-	-	-	0.3	0.3	-	-	-	0.7	0.7	-	-	-	1.3	1.3	-	-	-	-	-

K_c – coefficient used for the crops, plants, and tree; K_s – coefficient used for the rocks and bare soils; K_u – coefficient used for urban area; K_w – coefficient used for free water and marshes; K_{clc} – coefficient used for land cover in Emilia-Romagna.

For the particular locations, the daily ET_c investigation could have one more stage called the development season, that varies from crop to crop and place to place. For the regional assessment, due to the heterogeneity of the land cover and its growing characteristics, we assume only four stages of seasonality of ET_c. Thus, for initial season, mid-season, and late season the K_{clc} were asigned for each category of CLC2006 and for the cold season the K_{clc} were considered only for forest pattern of the land cover. This procedure is based on the premise that the hay and herbaceous vegetation suspend life functions due to heat energy lack (Allen et al. 1998) and the K_{clc} coefficient diminished with 1 in the cold season for beaved forest, while the constant K_{clc} remains active only for coniferous trees. The seasonal K_{clc} values taken into account for the Emilia-Romagna region are reported in the Table 2.

In the past, not all scientists agreed that areas without crops could be integrated into ET_c. The artificial surfaces and rocks were not considered like related areas for evapotranspiration (Celico, 1988), but studies subsequently made showed that urban areas, rocks, and bare soils could be recognized like a evaporation rate. Further, we integrate each category of land cover into calculation of ET_c. Depending of the type of plant, the climate region, and the latitude, we estimate for the K_{clc} by distinguishing three cases: (i) crop coefficient (K_c) for single crop in line with Allen et al. (1998), (ii) water evaporation coefficient (K_w) for free surface water using the coefficients suggested by Allen et al. (1998), (iii) rock and soil coefficient (K_s) for bare soils and rocks, and (iv) K_u for artificial areas. The K_s and K_u were chosen in conformity with Grimmond and Oke (1999) and Chicago was the reference city because has the appropriate latitude with Emilia-Romagna region.

The ET_c equation (Eq. 4) integrates the defined ratio of the K_{clc} to the reference ET_0. In the present work the seasonal K_{clc} was used to carry out the ET_c for different seasons based on seasonal ET_0 and the annual ET_c was obtained with the Equation (5).

$$\mathrm{ET_c} = \mathrm{ET_0 K_{clc}}[\mathrm{mm/month}] \qquad \text{(Eq.4)}$$

where:
ET_c = crop evapotranspiration
ET_0 = potential evapotranspiration
K_{clc} = land cover coefficient

$$\text{Annual } \mathrm{ET_c} = \mathrm{ET_{c\,ini}} + \mathrm{ET_{c\,mid}} + \mathrm{ET_{c\,end}} + \mathrm{ET_{c\,cold}} \; [\mathrm{mm}] \qquad \text{(Eq.5)}$$

where:
$ET_{c\,ini}$ = crop evapotranspiration related to initial stage
$ET_{c\,mid}$ = crop evapotranspiration related to mid stage
$ET_{c\,end}$ = crop evapotranspiration related to late stage
$ET_{c\,cold}$ = crop evapotranspiration related to cold stage

3.3.3. Actual crop evapotranspiration integrating Budyko equation

Budyko approach is important for water balance study, because it indicates if the energy is enough to evaporate the precipitation (Gerrits et al., 2009). Budyko equation (Eq. (6)) was used to find annual AET_c from the annual ET_c. This method is based on mean of annual input data of evapotranspiration, aridity index (Eq. 7) and precipitation and in present study the formula was applied on the raster maps.

$$\frac{\mathrm{AET_c}}{\mathrm{P_a}} = [\left(\varphi \tan\frac{1}{\varphi}\right)(1 - \exp^{-\varphi})]^{0.5} \qquad \text{(Eq.6)}$$

where:
AET_c= actual land cover evapotranspiration
P_a= total annual precipitation
φ = aridity index

$$\varphi = \frac{\mathrm{ET_c}}{\mathrm{P_a}} \qquad \text{(Eq.7)}$$

3.3.3. Spatial distribution of the ET_c

The spatial variation of climate data and ET_c calculation were mapped using ArcGIS 10.2.2 environment from ESRI. The wide functionality of ArcGIS software in the spatial data analysis and environment studies was confirmed by McCoy and Johnston (2002), Brown et al. (2005), Hadeel et al. (2010), Nistor and Petcu (2015). Holdaway (1996), Nusreta and Dugb (2012), Aalto et al. (2013) have used the Kriging interpolation for their climatological studies. Ordinary Kriging function is founded in Spatial Analyst Tools and was applied in the interpolation between calculated values and unknown values of temperature, precipitation, and ET_0 situated between meteorological stations. In this way, the unknown locations of the Emilia-Romagna territory were estimated through Kriging ordinary function. The Kriging ordinary is the simplest form of the Kriging interpolation and is based on a constant mean μ (Goovaerts, 1998). In this interpolation, the weights of the Kriging method take into account both the distance between the measured points and the overall spatial arrangement of the measured points. The spherical type was used for semivariogram model, variable types was chosen for the search radius settings in the Kriging ordinary procedure and the output cell size was set at 1000 m.

Based on vector data of CLC2006, the raster data of K_{clc} for four seasons was extracted using 'Conversion Tools' from ArcToolbox. Thus, the K_{clc} initial ($K_{clc\ ini}$), K_{clc} mid-season ($K_{clc\ mid}$), K_{clc} late season ($K_{clc\ end}$), and K_{clc} cold season ($K_{clc\ cold}$) raster maps with a 1000 m spatial resolution were carried out to estimate the seasonal ET_c. Using the 'Raster Calculator' function from Spatial Analyst Tools, we conduct the mathematical operations of seasonal ET_c, annual ET_c, and AET_c with raster maps.

4. Results and discussion

Using the methods presented above, the ET_c and AET_c maps of Emilia-Romagna region were drawn. The largest part of the study area indicates values of AET_c ranging from 500 to 600 mm which is spreading in the Po Plain and hilly area of the Emilia-Romagna region. This result corresponds to a mean annual AET_c of 557 mm and mean annual precipitation of 991 mm, especially in the lands occupied by the agricultural area and grasslands crops.

Figure 2 depicts the spatial distribution of mean annual temperature, mean annual precipitation, ET_0, and AET_0 in the Emilia-Romagna region. Based on Thornthwaite method, the mean monthy ET_0 was calculated for the period of 1991-2005. The annual ET_0 ranges from 535 mm at Bedonia station to 778 mm at Ferrara station. The mean values of annual ET_0 at the thirteen meteorological stations during 1991-2005 is 651 mm and exceed 300 mm in the mid-season (Figure 3).

The spatial distribution of seasonal K_{clc} are depicted in the Figure 4, which shows the maximum extension of highest values in the mid-season. The large area of highest values of K_{clc} (1.6) is found in the Northern Apennines, in the lands covered by the broad-leaved forest. In the Po Plain is found a significant area with a high value of K_{clc} (1.35) in the mid–season, mainly covered by non-irrigated arable land and complex cultivation pattern. Interestingly it was observed that in the cold season the K_{clc} has maximum values of 1 in the mountain area and some coastal zones due to continuous functionality of coniferous and broad-leaved forests and functionality reduction of agricultural crops and minimum values of evaporation in the artificial areas and free surface water.

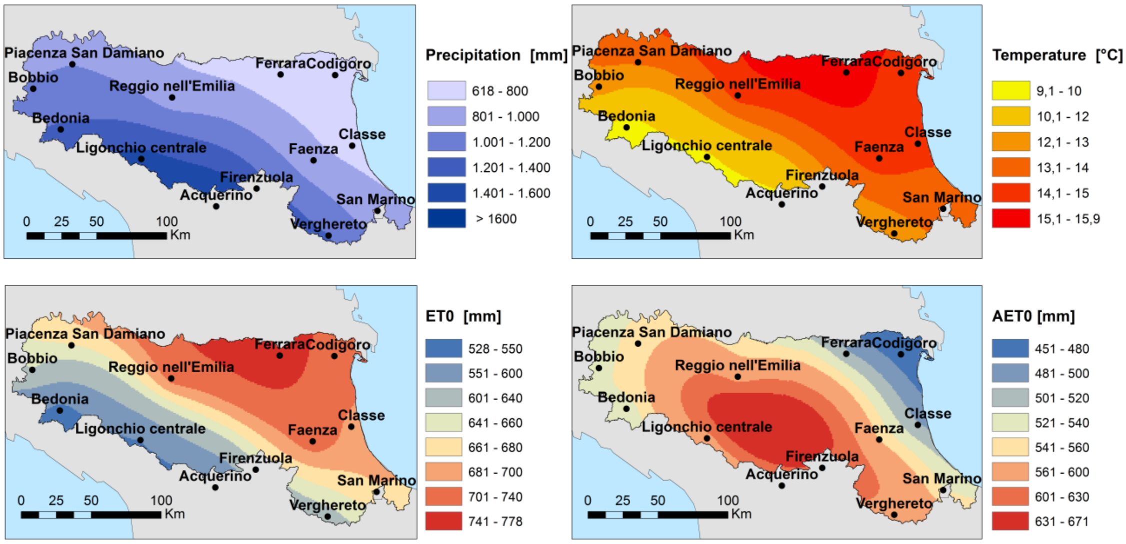

Figure 2 The mean annual areal precipitation, mean annual air temperature, annual ET_0, and annual AET_0 of the study area during 1991-2005.

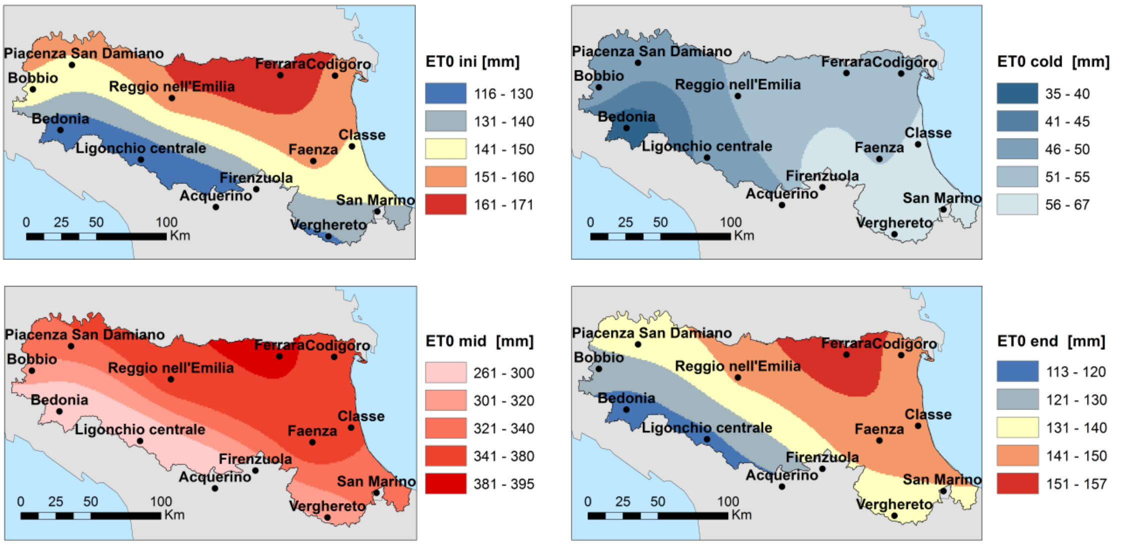

Figure 3 Spatial distribution of seasonal ET_0 on the Emilia-Romagna map during 1991-2005.

Figure 5 shows the seasonal ET_c maps of Emilia-Romagna region. The values of initial stage of ET_c ranging from 7 to 223 and are maximum in few areas of central and west part of the region. In the ET_c mid-season map is showed that the values exceed 600 mm due to high values of temperature, high values of ET_0 (over 300 mm), and high values of K_{clc} (1.351-1.6). The areas with highest $ET_{c\ mid}$ are in north of the region around Ferrara city and along the hilly area that extends at south of Reggio-Emilia, Parma, Modena, Bologna until to San Marino.

Interestingly, the spatial distribution of ET_c for the end-season, when the highest values reach 234 mm in the north part of Emilia-Romagna region and exceed in many places 190 mm in the hilly area cover by forest and near the Adriatic coast, in the areas of coastal lagoons.

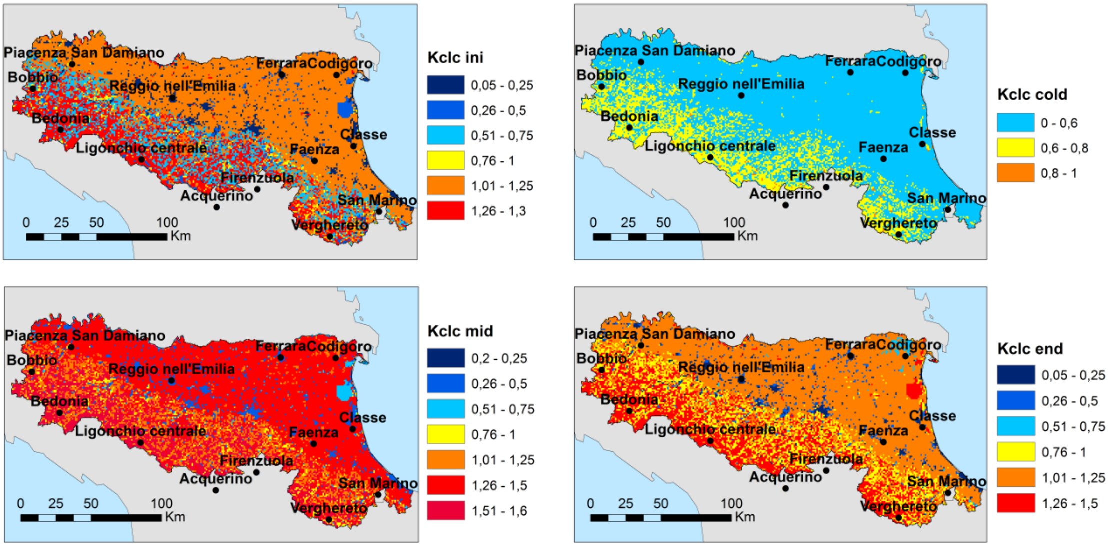

Figure 4 Spatial distribution of K_{clc} on the Emilia-Romagna map for the four stages.

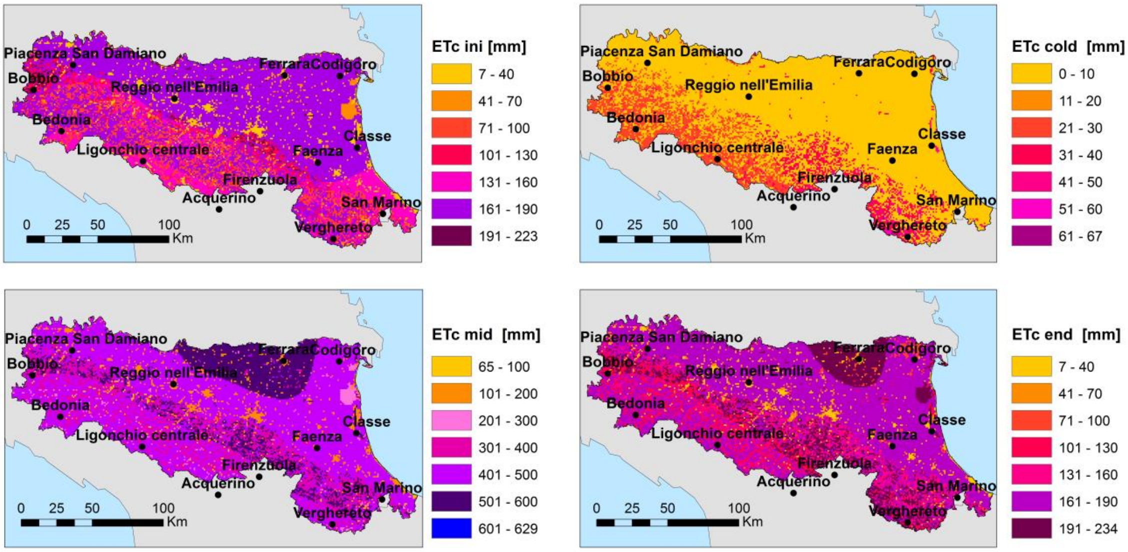

Figure 5 Spatial distribution of ET_c on the Emilia-Romagna map for the four stages.

In the cold season, more than half of Emilia-Romagna region had 0 value for the $ET_{c\ cold}$ from 1991 to 2005. The highest values reach 67 mm in the southeastern part of the region, in the Northern Apennines area. The spatial distribution of ET_c in the cold season is contrastly to ET_c from mid-season and shows the highest values of $ET_{c\ cold}$ in mountains area, even if the temperature and $ET_{0\ cold}$ are lower in this part of the region. These consequences are due to the presence of coniferous and mixed forest that have the high values of $K_{clc\ cold}$ and thus the $ET_{c\ cold}$ is higher in mountainous area during this period of the year than in Po Plain.

Using the Budyko approach, we extract the aridity index map from the annual ET_0 (Figure 6a) and annual ET_c (Figure 6b) integrating the precipitation raster map. This parameter is important for the determination of AET_0 and AET_c. The high values of aridity index extracted from ET_0 exceeds

1.1 in the northeast part of the region. The low values of aridity index were identified in south of the region around Acquerino and Ligonchio centrale stations where the annual ET_0 has low values and precipitations has high values. The aridity index calculated with annual ET_c reaches the maximum values of 1.69 in the northeast part of the region, near the Codigoro and Ferrara stations. The minimum values were founded in the urban area and in some places from Northern Apennines. The Pearson correlation was pointed out between aridity index calculated with annual ET_0 for each meteorological station and mean annual air temperature. The correlation value is 0.92 and indicates a high correlation between both parameters on whole Emilia-Romagna region. Figure 6c highlights the annual ET_c map of Emilia-Romagna region and reflects the ability to evapotranspiration of land cover in this region. The values over 1000 mm were depicted in the north and northeastern part of Emilia-Romagna, while in the south and southwestern part the ET_c ranges between 400 to 800 mm. The urban areas registered the lower values of ET_c, typically below 200 mm.

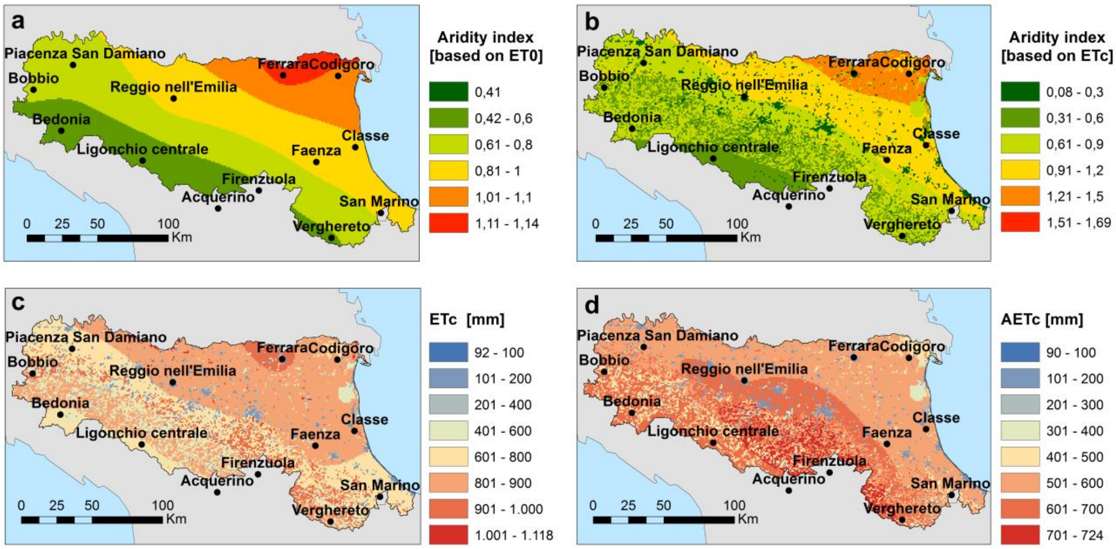

Figure 6 a. Aridity index map of Emilia-Romagna computed with ET_0. **b.** Aridity index map of Emilia-Romagna computed with ET_c. **c.** Spatial distribution of annual ET_c on the Emilia-Romagna map. **d.** Spatial distribution of annual AET_c on the Emilia-Romagna map.

Integrating the annual ET_c in the Budyko equation, the raster map of AET_c was derived for Emilia-Romagna region that accounts the land cover evapotranspiration. Figure 6d shows the spatial variation of AET_c based on aridity index extracted from annual ET_c and annual precipitation raster data. A high deficit of water was estimated in the southcentral area of Emilia-Romagna region, where the values of AET_c rise up to 700 mm. In the Po Plain are identified values that range from 500 mm to 700 mm, while in the Northern Apennines the AET_c ranges from 300 mm to 500. The low values of AET_c were depicted in the urban areas and northeastern extremity of the region near the Codigoro station where the precipitation are lower.

One of the main goal of this study was to assess the evapotranspiration of land cover from Emilia-Romagna region. Looking at representation of the spatial distribution of annual ET_c and annual AET_c, we expected to see the highest values in the central and north part of the region. The mid-season and end season show the highest ratio of K_{clc}. As a concequence, the $ET_{c\ mid}$ values are rising in this annual period. We did not expect that in end season the $ET_{c\ end}$ values of mountain area to be so high compared with initial season. Analysing the high values of ET_c during the mid-season and end season with lower values of precipitation in the same period of year we concludes that climate and land cover have a negative impact for groundwater recharge, ecosystems, and agricultural activities. From the both aridity index maps resulted that in the plain area the water irrigation is required because of water deficit. The high values of annual ET_c have significant importance for recharge area of aquifers, springs flow discharge and for the water surplus of the region.

The main limitation of our research was that we used the empirical formulas for ET_c and we didn't have field data measurements from 1991-2005 period. The measurement made by pan or lysimeter was not included in our research. Actually, we cannot check the crop coefficient ratio in a different location and different types of crop over the Emilia-Romagna region. Moreover, if we check the ratio values of one type of land cover in a certain field location could be not well to apply the same ratio for other location for the same region, because the properties of measurement crop with pan reflect the ratio in particular locations, but not the overall tendency. For this reason we adapt the standard values from FAO-56 Paper. Clearly, even if the K_{clc} assigned for each category of land cover is correct from a standard point of view, the ET_c of each crop could be slightly filled with small errors. These things do not affect the overall results at regional scale because the final map of AET_c is based not only on K_{clc}, but also on annual precipitation and annual ET_c as well. However, from the findings of those limited trends, a clear data set of recent climate change and CLC2006 can be useful for future scenarios. Therefore, by using our method we did not interpolated the measurements of ET_c points but interpolated only the basic climatic data that were introduced further in the analysis.

A full treatment of K_{clc} and climate variation is a complicated operation, due to the large number of variables. For example, the presence of soils, temperature, precipitation, and humidity affect in different ways the ET_c related to the same land cover that exists in different locations. The possibility to offer an integrated methodology at regional scale for Emilia-Romana using GIS, climate data, and CLC2006 is an exciting proposition**.**

5. Conclusions

The climate and environmental study carried out by the spatial distribution of the land cover evapotranspiration provided useful information for agricultural, hydrology, and climatology interest. Based on the proposed methodology and obtained results the follows conclusions may be drawn:

- Applying the Ordinary Kriging function, the temperature, precipitation, and ET_0 calculated for 13 wethear stations were interpolated and the unknown values from Emilia-Romagna region were located.
- Integrating the seasonal appropriate K_{clc} ratio into the ET_c calculation of Emilia-Romagna region and using the seasonal raster data of $ET_{0\ ini}$, $ET_{0\ mid}$, $ET_{0\ end}$, $ET_{0\ cold}$, the land cover evapotranspiration at regional scale for four seasons were carried out.
- Using the GIS applications, the spatial distribution of annual ET_c and annual AET_c maps were drawn. The ET_c register the highest values during the mid-season in the Po Plain area, near Ferrara station due to high values of temperature and also for the K_{clc} values too.
- To the interpretation of the Budyko approach and aridity index the water deficit areas were calculated and identified for the Emilia-Romagna region related to climatic mean annual values from 1991 to 2005 and CLC2006.

- The accuracy of the annual ET_c is affected by the local conditions where the humidity and wind speed were not considered in present paper. This was due to the extremely complicated procedure of interpolation that is very sensitive from place to place.

In conclusion, the combination of empirical equations and spatial calculations of available data and the adapted FAO-56 standard approach, together with GIS tools, represent a valuable method to compute the ETc at regional scale of Emilia-Romagna and may be easily applicable to other regions around the world.

Acknowledgements
This paper is made and published under the aegis of the Research Institute for Quality of Life, Romanian Academy, as a part of programme co-funded by the European Union within the Operational Sectorial Programme for Human Resources Development through the project for Pluri- and interdisciplinary in doctoral and post-doctoral programmes, Project Code: POSDRU/159/1.5/S/141086.

References

Aalto J., Pirinen P., Heikkinen J. et al. 2013. Spatial interpolation of monthly climate data for Finland: comparing the performance of kriging and generalized additive models. *Theor. Appl. Climatol*. 112: 99-111.

Aguilera H., Murillo J. M. 2009. The effect of possible climate change on natural groundwater recharge based on a simple model: a study of four karstic aquifers in SE Spain. *Environmental Geology* 57(5): 963-974.

Allen R. G., Pereira L. S., Raes D. et al. 1998. *Crop evapotranspiration: guidelines for computing crop water requirements*. FAO Irrigation and Drainage Paper 56, Rome, 300 pp.

Allen R. G. 2000. Using the FAO-56 dual crop coefficient method over an irrigated region as part of an evapotranspiration intercomparison study. *Journal of Hydrology* 229: 27-41.

Arpa Emilia-Romagna. 2015. Tabelle climatologiche 1961-2005. http://www.arpa.emr.it/. [Accessed on May 8, 2015]

Bachu S., Adams J. J. 2003. Sequestration of CO2 in geological media in response to climate change: capacity of deep saline aquifers to sequester CO2 in solution. *Energy Conversion and Management* 44: 3151-3175.

Brouyère S., Carabin G., Dassargues A. 2004. Climate change impacts on groundwater resources: modelled deficits in a chalky aquifer, Geer basin, Belgium. *Springer-Verlag Hydrogeology Journal* 12: 123-134.

Brown D. G., Riolo R., Robinson D. T. et al. 2005. Spatial process and data models: Toward integration of agent-based models and GIS. *Journal of Geographical Systems* 7: 25-47.

Campos G. E., Moran M. S., Huete A. et al. 2013. Ecosystem resilience despite large-scale altered hydroclimatic conditions. Macmillan Publishers. *Nature* 494: 349-353.

Celico P. 1988. *Hydrogeological prospecting*. Liguori Press 2nd edition, Napoli. (in Italian)

Chen S. B., Liu Y. F., Thomas A. 2006. Climatic change on the Tibetan plateau: potential evapotranspiration trends from 1961 to 2000. *Clim. Chang*. 76: 291-319.

Collins D. N. 2008. Climatic warming, glacier recession and runoff from Alpine basins after the Little Ice Age maximum. *Annals of Glaciology* 48(1): 119-124.

Dong P., Wang C., Ding J. 2013. Estimating glacier volume loss used remotely sensed images, digital elevation data, and GIS modelling. *International Journal of Remote Sensing* 34(24): 8881-8892.

Goovaerts P. 1998. Ordinary cokriging revisited. *Math. Geol*. 30(1): 21–42.

Gao G., Chen D., Xu C. Y. et al. 2007. Trend of estimated actual evapotranspiration over China during 1960–2002. *J. Geophys. Res*. 112(D11120), doi:10.1029/2006JD008010.

Gao G., Xu C. Y., Chen D. et al. 2012. Spatial and temporal characteristics of actual evapotranspiration over Haihe River basin in China. *Stoch. Environ. Res. Risk. Assess*. 26: 655-669.

Gerrits A. M. J., Savenije H. H. G., Veling E. J. M. et al. 2009. Analytical derivation of the Budyko curve based on rainfall characteristics and a simple evaporation model. *Water Resour. Res*. 45(W04403), doi: 10.1029/2008WR007308.

Gowda P. H., Chavez J. L., Colaizzi P. D. *et al*. 2008. ET mapping for agricultural water management: present status and challenges. *Irrig. Sci*. 26: 223-237.

Grimmond C. S. B., Oke T. R. 1999. *Evapotranspiration rates in urban areas, Impacts of Urban Growth on Surface Water and Groundwater Quality*. Proceedings of IUGG 99 Symposium HSS. Birmingham, July J999. IAHS Publ. no. 259: 235-243.

IPCC. 2001. *Climate Change 2001: The Scientific Basis*. Contribution of Working Group I to the Third Assessment Report of the Intergovernmental Panel on Climate Change [Houghton J. T., Ding Y., Griggs D. J. et al. (eds.)]. Cambridge University Press, Cambridge, United Kingdom and New York, NY, USA, 881 pp.

IPCC. 2007. *Climate Change 2007: Impacts, Adaptation and Vulnerability*. Contribution of Working Group II to the Fourth Assessment Report of the Intergovernmental Panel on Climate Change [Parry M. L., Canziani O. F., Palutikof J. P. et al. (eds.)] Cambridge University Press, Cambridge, UK 976 pp.

ISTAT (Istituto nazionale di statistica). 2014. *Annuario statistico italiano 2014*, ISBN 978-88-458-1817-2 (online), Roma.

Jiménez Cisneros B. E., Oki T., Arnell N. W. et al. 2014. *Freshwater resources. In: Climate Change 2014: Impacts, Adaptation, and Vulnerability. Part A: Global and Sectoral Aspects.* Contribution of Working Group II to the Fifth Assessment Report of the Intergovernmental Panel on Climate Change [Field C. B., Barros V. R., Dokken D. J. et al. (eds.)]. Cambridge University Press, Cambridge, United Kingdom and New York, NY, USA, 229-269.

Hidalgo H. G., Das T., Dettinger M. D. et al. 2009. Detection and attribution of streamflow timing changes to climate change in the western United States. *Journal of Climate* 22(13): 3838-3855.

Hadeel A. S., Jabbar M. T., Chen X. 2010. Application of remote sensing and GIS in the study of environmental sensitivity to desertification: a case study in Basrah Province, southern part of Iraq. *Appl. Geomat*. 2: 101-112.

Holdaway R. M. 1996. Spatial modeling and interpolation of monthly temperature using kriging. *Climate Research* 6: 215-225.

Kottek M., Grieser J., Beck C. et al. 2006. World Map of the Köppen-Geiger climate classification updated. *Meteorol. Z*. 15(3): 259-263.

Kousari M. R., Zarch M. A. A., Ahani H. et al. 2013. A survey of temporal and spatial reference crop evapotranspiration trends in Iran from 1960 to 2005. *Climatic Change* 120: 277-298.

Kurnik B., Kajfež-Bogatajb L., Horionc S. 2014. An assessment of actual evapotranspiration and soil water deficit in agricultural regions in Europe. *Int. J. Climatol*. doi: 10.1002/joc.4154.

Loàiciga H. A., Maidment D. R., Valdes J. B. 2000. Climate-change impacts in a regional karst aquifer, Texas, USA. *Journal of Hydrology* 227: 173-194.

McCabe J. G. J., Wolock D. M. 1991. Detectability of the effects of a hypothetical temperature increase on the Thornthwaite moisture index. *J. Hydrol*. 125: 25-35.

McCoy J., Johnston K. 2002. *Using ArcGIS™ Spatial Analyst, GIS by ESRI.* Printed in the United States of America.

Mojid M. A., Rannu R. P., Karim N. N. 2015. Climate change impacts on reference crop evapotranspiration in North-West hydrological region of Bangladesh. *Int. J. Climatol*. doi: 10.1002/joc.4260.

Nistor M. M., Petcu I. M. 2015. Quantitative analysis of glaciers changes from Passage Canal based on GIS and satellite images, South Alaska. *Applied Ecology and Environmental Research* 13(2): 535-549.

Nusreta D., Dugb S. 2012. Applying the Inverse Distance Weighting and Kriging methods of the spatial interpolation on the mapping the annual precipitation in Bosnia and Herzegovina, [Seppelt R., Voinov A. A., Lange S. et al. (eds.)] International Congress on Environmental Modelling and Software, Managing Resources of a Limited Planet, Sixth Biennial Meeting, Leipzig, Germany.

Oerlemans J. 2005. Extracting a Climate Signal from 169 Glacier Records. *Science* 308: 675-677.

Parmesan C., Yohe G. 2003. A globally coherent fingerprint of climate change impacts across natural systems. *Nature* 421(2): 37-42.

Piao S., Ciais P., Huang Y. et al. 2010. The impacts of climate change on water resources and agriculture in China. *Nature* 467(7311): 43-51.

Prăvălie R. 2014. Analysis of temperature, precipitation and potential evapotranspiration trends in southern Oltenia in the context of climate change. *Geographia Technica* 9(2): 68-84.

Prăvălie R., Sîrodoev I., Peptenatu D. 2014. Detecting climate change effects on forest ecosystems in Southwestern Romania using Landsat TM NDVI data. *Journal of Geographical Sciences* 24(5): 815-832.

Rahardjo H., Satyanaga A., Leong E. C. 2012. Effects of flux boundary conditions on pore-water pressure distribution in slope. *Eng. Geol*. 165: 133-142.

Rosenberry D. O., Winter T. C., Buso D. C. et al. 2007. Comparison of 15 evaporation methods applied to a small mountain lake in the northeastern USA. *J. Hydrol*. 340: 149-166.

Shahgedanova M., Stokes C. R., Gurney S. D. et al. 2005. Interactions between mass balance, atmospheric circulation, and recent climate change on the Djankuat Glacier, Caucasus Mountains, Russia. *Journal of Geophysical Research* 110(D4): 1-12.

Shaver G. R., Canadell J., Chapin III F. S. *et al*. 2000. Global Warming and Terrestrial Ecosystems: A Conceptual Framework for Analysis. *Oxford Journals BioScience* 50(10): 871-882.

Stavig L., Collins L., Hager C. et al. 2005. The effects of climate change on Cordova, Alaska on the Prince William Sound. *Alaska Tsunami Papers*. Publishing Web. https://seagrant.uaf.edu/nosb/papers/2005/cordova-nurds.html. [Accessed on April 23, 2014]

Stocks B. J., Fosberg M. A., Lynham T. J. et al. 1998. Climate change and forest fire potential in Russian and Canadian boreal forests. *Climatic Change* 38: 1-13.

Thornthwaite C. W. 1948. An approach toward a rational classification of climate. *Geogr Rev*. 38: 55-94.

The Canadian Centre for Climate Modelling and Analysis. 2014. The First Generation Coupled Global Climate Model Publishing Web. http://www.ec.gc.ca/ccmac-cccma/default.asp?lang=En&n=540909E4-1. [Accessed on March 20, 2015]

Xie X., Li Y. X., Li. R. et al. 2013. Hyperspectral characteristics and growth monitoring of rice (Oryza sativa) under asymmetric warming. *International Journal of Remote Sensing* 34(23): 8449-8462.